Presented at the 29th ASME Wind Energy Symposium (49th AIAA Aerospace Sciences Meeting)
4-7 January 2011, Orlando, Florida, USA

Design, Fabrication, Assembly and Initial Testing of a SMART Rotor[1]

Dale Berg[2], Jon Berg[3], David Wilson[3], Jon White[3], Brian Resor[3] and Mark Rumsey[3]
Sandia National Laboratories[4], Albuquerque, NM 87185-1124

Sandia National Laboratories has designed and built a full set of three 9m blades (based on the Sandia CX-100 blade design) equipped with active aerodynamic blade load control surfaces on the outboard trailing edges. The design and fabrication of the blades and active aerodynamic control hardware and the instrumentation are discussed and the plans for control development are presented.

I. Introduction

Reducing ultimate and oscillating (or fatigue) loads on wind turbine rotors can lead to reductions in loads on other turbine components such as the drive train, gearboxes, generators and towers, resulting in large reductions in both the initial capital costs and the maintenance costs. These cost reductions, in turn, can lead to decreases in the resultant turbine cost of energy. With the ever increasing size of wind turbine blades and the corresponding increase in non-uniform loads along the span of those blades, the need for more sophisticated load control techniques has resulted in increased interest in the use of aerodynamic control devices (with associated sensors and control systems) distributed along each blade to provide feedback load control (often referred to in popular terms as 'smart structures' or 'smart rotor control'). A recent review of concepts and feasibility and an inventory of design options for such systems have been performed by Barlas and van Kuik at Delft University of Technology (TUDelft)[1]. Active load control utilizing trailing edge flaps or deformable trailing edge geometries (referred to here as Active Aerodynamic Load Control or AALC) is receiving significant attention, because of the direct lift control capability of such devices and recent advances in smart material actuator technology. Researchers at TUDelft[2-3], Risø/Danish Technical University Laboratory for Sustainable Energy (Risø/DTU)[4-10] and Sandia National Laboratories (SNL)[11-17] have been very active in this area over the past few years.

The SNL work has focused on performing extensive simulations of AALC on several turbine configurations and has analyzed the simulation results to estimate the fatigue damage reduction on the rotor and gearbox and the cost-of-energy benefits of integrating trailing edge technology into the tip region of the turbine blades. These simulation results show the potential for significant impacts on fatigue damage and cost of energy, but experimental data is badly needed to confirm the simulation-based analyses. To the best of our knowledge, no research group has yet built and field tested a smart rotor control blade set.

SNL operates a small test turbine located on the U.S. Department of Agriculture (USDA) Agricultural Research Station at Bushland, TX, just west of Amarillo. We have just built a set of 9m blades for that turbine that will, when modifications are completed, be equipped with 20% chord flaps over the outer 2m of the blade span. The design and fabrication of that blade set and our plans for testing it are the subjects of this paper.

---

[1] This paper is declared work of the U.S. Government and is not subject to copyright protection in the United States.

[2] Principal Member of Technical Staff, Wind Energy Technology Department, Mail Stop 1124, AIAA Associate Fellow

[3] Member of Technical Staff, Wind Energy Technology Department, Mail Stop 1124, AIAA Member

[4] Sandia is a multiprogram laboratory operated by Sandia Corporation, a Lockheed Martin Company, for the United States Department of Energy's National Nuclear Security Administration under contract DE-AC04-94AL85000.

II. Blade Design

While there are many questions associated with the use of AALC devices that must be answered with field testing experience and experimental data, we are restricting the general goals for this particular effort to:

- Develop the procedures required for validating the structural model of an operating wind turbine incorporating AALC (System ID).
- Evaluate/demonstrate numerous aerodynamic and structural sensor systems to determine those that offer the most benefit as signal inputs for the AALC controllers.
- Evaluate the control authority of one particular type of AALC device.
- Begin to acquire the experimental data that are required to valídate the simulation tools.

Note that we are not designing the optimal rotor for integration of AALC control capability. In order to save time and money, we decided to modify the existing CX-100 blade design[18], rather than design a new blade from scratch, thus minimizing the amount of analysis that was required to ensure the new design could withstand the operating loads. The CX-100 was designed to withstand IEC wind class IIB extreme conditions, but we are restricting SMART operation to normal IEC Category IIB conditions. Our analyses indicate that the SMART blade loads with the additional loads due to the AALC device operations will remain below the design loads for the CX-100. Thus, so long as the SMART blade stiffnesses are at least as high as those of the CX-100, the strains will not exceed those experienced by the CX-100 at design load conditions. We therefore restricted our structural analyses to only those required to ensure that the modified blade stiffnesses were at least as high as those for the original blade.

The CX-100 blade is a well-known and well-characterized 9m blade. A cross-sectional sketch of a typical outboard blade section may be seen in Figure 1. The original blade design incorporated a single fiber glass/balsa core shear web with carbon spar caps and skins of double-bias fiberglass sandwiching a ¼ inch thick balsa panel. For the skins aft of the shear web, the skin laminate stack comprised a gel coat at the outer surface, a mat, then a single layer of double-bias fiber glass, a balsa core, and a second, inner layer of double-bias fiber glass. In the following discussion, keep in mind that blade station 0 is the blade root end of the blade and station 9.0 is at the blade tip.

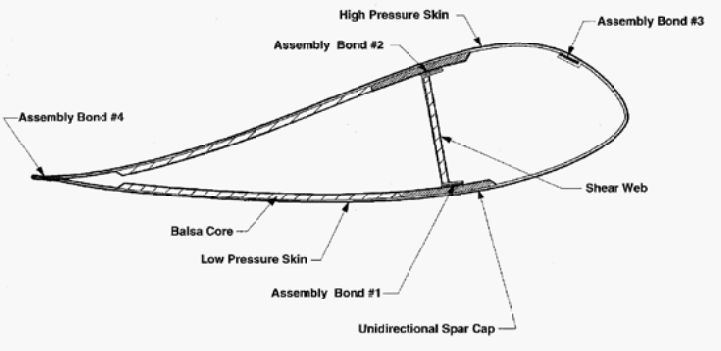

Figure 1 Outboard Cross Section of a Typical 100 kW Blade (Courtesy of TPI Composites)

The earlier simulation studies have shown that the most effective location for AALC devices is on the outer portion of the blade span, so the SMART blades incorporate a cutout of the trailing-edge section extending for approximately 20% of the outer blade span to accommodate mounting of active aerodynamic control devices in that area. In order to accommodate the 20% chord flaps (and the related support structure) that simulations indicate will exert sufficient control authority, this cutout extends 40% of chord forward of the trailing edge at 7.029m (the inboard end) and linearly expands to 50% of chord at 8.857m (the outboard end). This cutout does not extend to the tip of the blade – the outer 14.3cm (one tip chord length) of the trailing edge is left intact to minimize the impact of the blade tip vortex on the performance of the AALC device.

Removing this amount of material from the CX-100 blade would have very large impacts on the structural properties of the blade in the outboard region – the lead-lag, flap and torsional stiffnesses would all be significantly reduced. In order to minimize or eliminate those reductions, the SMART blade design replaces the outer layer of glass double-bias laminate in both the high pressure and low pressure skins with a double layer of carbon fiber double-bias laminate. As shown on Figure 2, the carbon material starts at the trailing edge at 6m and reaches the leading edge at about 6.5m, with the transition line between glass and carbon following the bias fiber direction of 45°. The inboard edges of the two carbon layers overlap (by 75mm for the outer layer and 150mm for the inner layer) the outboard edge of the fiber glass layer in the transition region to efficiently transfer the skin loads between the two skin materials.

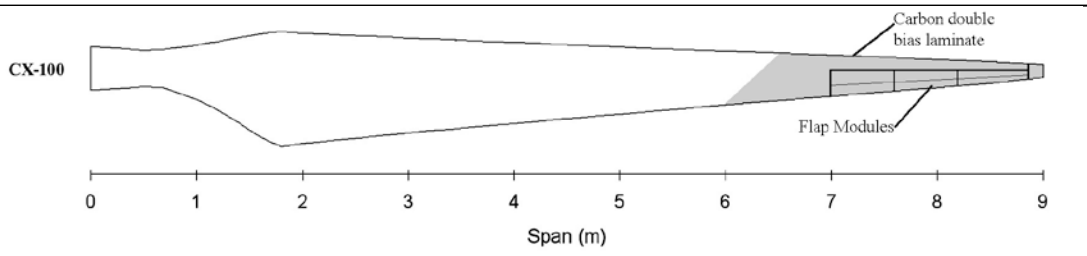

Figure 2 Planform of the CX-100 and SMART Blades

The CX-100 shear web ends at approximately 8m. For the SMART design, we have added a second shear web between 7.0m and 8.8m, mounted somewhat aft of the original shear web. This aft shear web provides a mounting point for the active aero modules, facilitates the transfer of the associated loads toward the root of the blade, and helps to maintain torsional stiffness. We have also added a single rib at the inner end of the cut-out region to help transfer the loads from the aft shear web to the main shear web. The aft shear web and cutout effectively reduce the aft panel size and eliminate any concerns of buckling outboard of 7.0m, so we have removed the balsa from the skins in this area, as well. The aft shear web and rib additions are illustrated in Figure 3.

We used a modified version of the NREL PreComp code[19] to compare blade stiffnesses of the original CX-100 blade and the SMART blade. Figure 4 shows that the addition of the carbon fiber laminate effectively compensates for the loss of stiffness due to removing the trailing edge material to accommodate the aerodynamic control modules.

The SMART blades were fabricated by TPI at their Rhode Island plant in June, 2010, using their original CX-100 molds and their standard vacuum infusion process utilizing epoxy resin. Extensive instrumentation (described in a later section of this paper) was installed and the blades were closed in early October 2010. Following some final surface finish work, they were shipped to Albuquerque, where SNL personnel are now modifying them to the final SMART configuration by cutting out the trailing edges and fabricating and installing the aft shear webs and inboard ribs (both vacuum-infused parts utilizing epoxy resin and 2 layers of carbon double-bias laminate on either side of a ½" marine-grade birch plywood core).

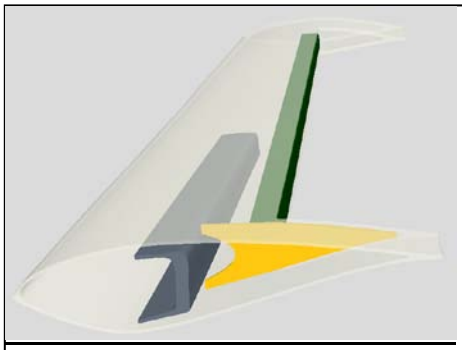

Figure 3 Modifications to the Outboard Blade to Accommodate Trailing Edge Load Control Modules. Dark Gray is Existing Shear Web, Green is Retrofit Aft Shear Web, Yellow is Retrofit Rib (View is Looking Outboard From 7.0 m).

III. Active Aerodynamic Control Devices

The aerodynamic control devices on this initial demonstration unit are 20% chord conventional flaps with +/- 20° maximum deflection. We elected the conventional flaps not because they will provide the best possible performance, but because our primary objective in this project is to build and fly a set of SMART blades. By using flaps we saved the development time and cost that would be required to miniaturize other potential control devices such as microtabs or morphing trailing edge flaps.

There are three independent control surfaces on each blade. The reasoning behind this design decision is multifaceted. First of all, space is limited at the blade tip and it is evident that the "muscle" required to drive a single flap covering 20% of blade span is more than what can be packed into any one location. In addition, independent actuation of multiple flaps is desirable, both for initial testing and for future research into distributed control (the test plan calls for gradually increasing the control capability to make sure the turbine response is well understood before the full control capability is exercised). Finally, our chosen manufacturing method naturally resulted in modules of a certain size. Given the complex geometry and our need to have the ability to quickly make design iterations, rapid prototyping technology was the clear choice for fabrication. Our in-house capability is limited to parts with the largest dimension being about one foot; each flap module consists of two of these1-foot pieces joined together. This necessitated having three modules per blade to obtain the desired length of flap.

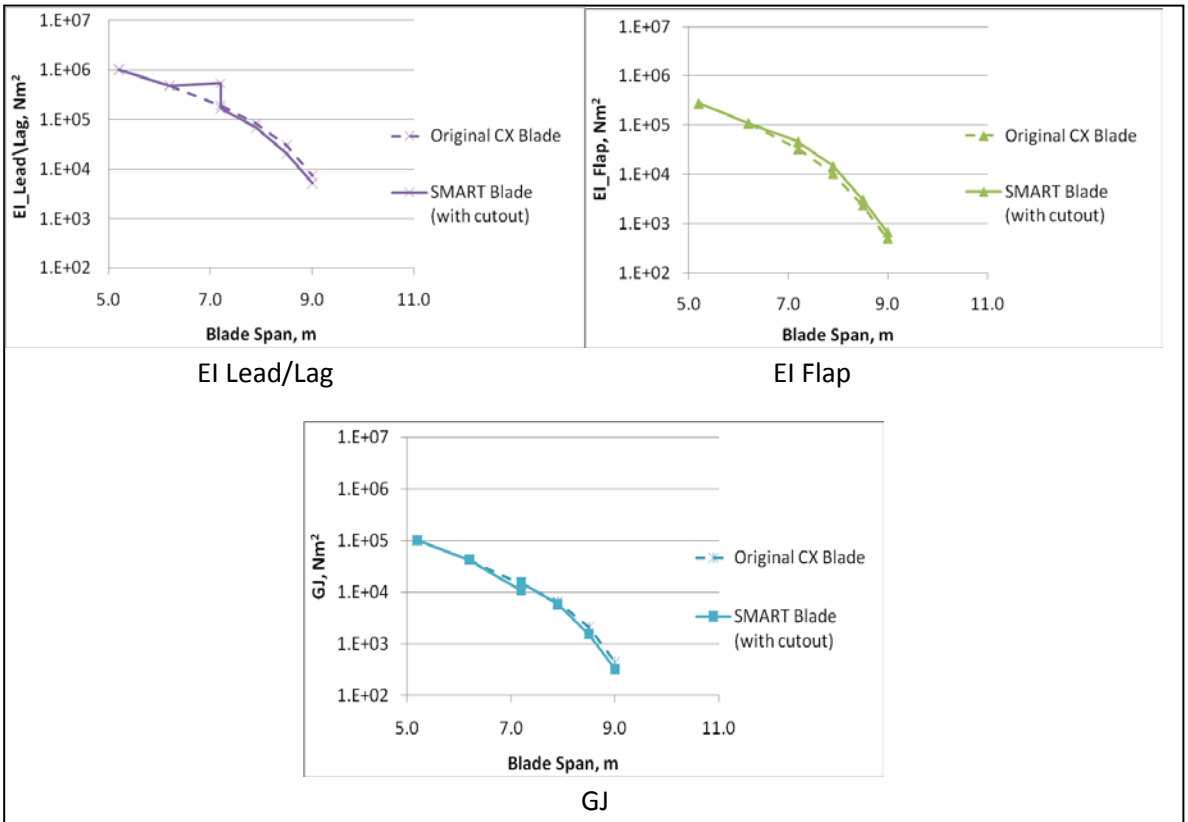

Figure 4 Comparison of CX-100 and SMART Blade Stiffness Values.

There are three independent control surfaces on each blade. The reasoning behind this design decision is multifaceted. First of all, space is limited at the blade tip and it is evident that the "muscle" required to drive a single flap covering 20% of blade span is more than what can be packed into any one location. In addition, independent actuation of multiple flaps is desirable, both for initial testing and for future research into distributed control (the test plan calls for gradually increasing the control capability to make sure the turbine response is well understood before the full control capability is exercised). Finally, our chosen manufacturing method naturally resulted in modules of a certain size. Given the complex geometry and our need to have the ability to quickly make design iterations, rapid prototyping technology was the clear choice for fabrication. Our in-house capability is limited to parts with the largest dimension being about one foot; each flap module consists of two of these1-foot pieces joined together. This necessitated having three modules per blade to obtain the desired length of flap.

The design of each flap module consists of two main pieces: (1) a base piece that houses the motor and mounts to the blade and (2) the flap itself that is attached to the base by a hinge as illustrated in Figure 5. The center module of the three modules on each blade also includes channels running to surface pressure taps and a mounting space for two accelerometers. To reduce weight and minimize the impact of the modules on the structural dynamic response of the blade, the base and flap were hollowed out as much as possible without sacrificing structural integrity (the skin thickness of the flap is approximately 0.06" and the wall thickness of the base is approximately 0.20"). In addition, the flap center of gravity was moved as far forward as possible without adding mass, in order to minimize the possibility of flap flutter. Both the flap and the base are fabricated using a rapid prototyping printer by building up layers of P400 ABS plastic. This plastic has a density of 1.05 g/cm^3 and a tensile strength of 5000 psi (34.4 MPa).

Two designs have been considered for the linkage between the motor and the flap. The first, seen in Figure 5, uses two pulleys and a timing belt with a belt-tension device. The second design uses control horns and dual rigid push/pull rods. The belt design has the advantage of being totally enclosed within the surface of the module; however, there is some concern over lack of stiffness in the mechanism when the loading direction reverses. The control horn/rod design was developed to address that concern. The disadvantage to this design is that some of the mechanism extends beyond the blade surface. Views of both designs are shown in Figure 6.

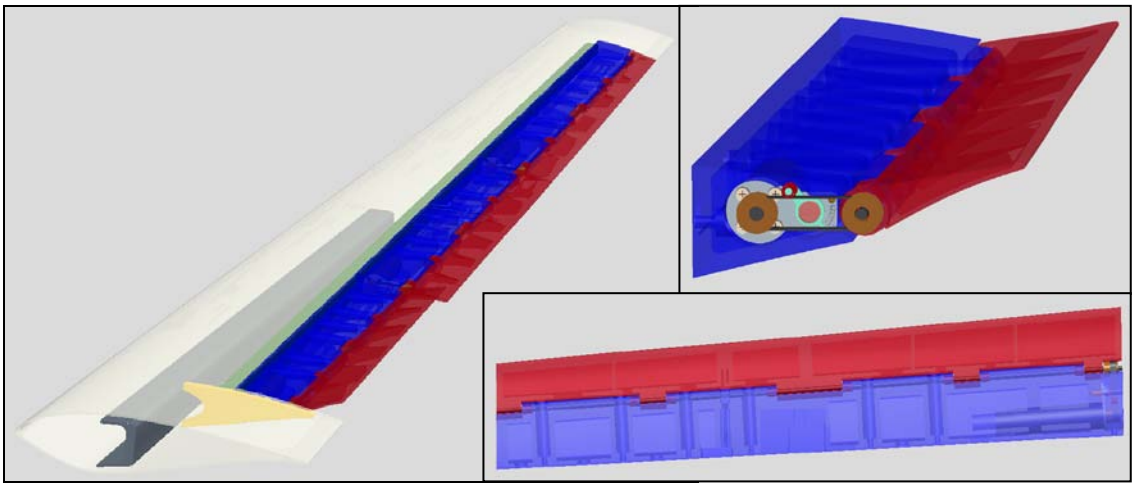

Figure 5 Trailing Edge Flap Module Design. Red is the Active Flap and Blue is the Base Support Structure.

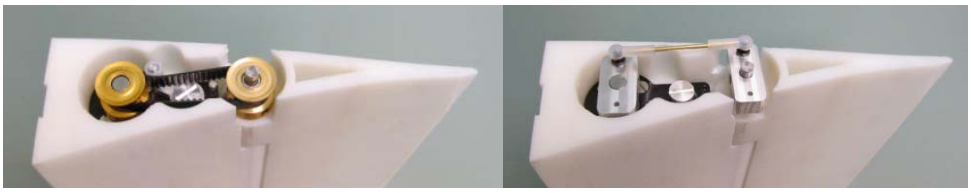

Figure 6 Actuator Designs; (a) Belt Driven, (b) Control Horn Driven (Prototype).

We wanted to create control surfaces that, when not deflected, closely match the original CX-100 profiles. In order to determine those profiles, we contracted Sandia's measurement group to use their 3-axis coordinate measurement machine (CMM) to scan one of our existing CX-100 blades at a number of span locations, approximately 10cm apart. The CMM was large enough to accommodate a piece of the blade about 2 meters long. The measured surface profiles were modified somewhat to obtain a sharper trailing edge on the flaps and remove some of the manufacturing irregularities observed in this particular blade before they were used to define the flap profiles.

The drive motors were selected by considering the required torque and desired actuation rate. The most inboard module (from span 7.03m to 7.64m) experiences the largest moment about the flap hinge line. Under *static* aerodynamic loading, this module experiences a hinge moment of 1.78N-m at 20° flap deflection and 20° angle of attack. Additional torque is required to accelerate the flap to the desired speed and overcome inertial loading and unsteady aerodynamic loading effects. We estimated that accounting for these three items results in a total required torque of 3.2N-m. We also estimated that an actuation rate of 300deg/s or higher is adequate to achieve fully unsteady aerodynamics effects. Based on these torque and speed requirements, we selected the Faulhaber series 2642W024CR motor with a 26/1S series gearhead having a reduction ratio of 66:1. The torque-speed operating range of this motor/gearhead is illustrated in Figure 7 (the red curves are a few example sinusoidal flap motions, including 0° - 20° at 5Hz, -20° - 0° at 5Hz, ±10° at 5Hz, ±5° at 10Hz and ±2.5° at 20Hz). A Faulhaber series IE3-512L magnetic encoder was selected to provide position feedback. This encoder has a line driver which allows the encoder signal to be transmitted down the length of the blade to a motor position controller located in the hub. We chose to use the Maxon EPOS2 24/5 positioning control unit to drive each motor. This motor driver can supply 5 amps continuously and 10 amps intermittently at 24 volts, while the motor should require less than 2 amps for most flap motions and loading conditions.

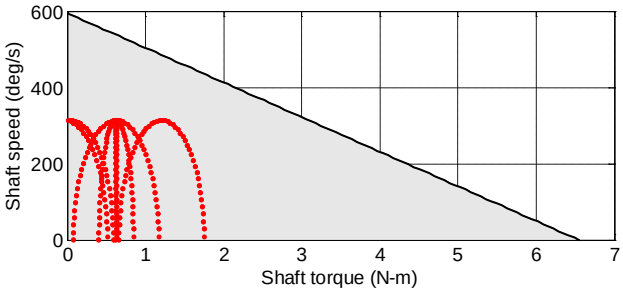

Figure 7. Flap Motor Operating Range (the Gray Area Under the Torque-speed Line). The Red Curves are Examples of a Few Sinusoidal Motions (Static Aerodynamics Only).

IV. Blade Instrumentation

A utility scale horizontal axis turbine is a highly coupled dynamic structure due to its slender geometry and flexibility; any force applied to any part of the rotor generates a response through all subcomponents. Localized approaches of a modeling, observing and controlling only a single rotor blade or even a specific spanwise location on that blade have the potential to create responses on the other rotor blades or other turbine components that lead to overall instabilities, increasing turbine fatigue and/or reducing performance. In the SMART rotor effort, we are concentrating on very accurately modeling, observing and controlling the entire rotor to produce the desired overall turbine performance and/or reliability benefit.

Sandia has developed several new sensor optimization strategies and state estimators to maximize the performance of the overall controls observer (a measurement or quantity computed from measurements) and minimize the number of sensors required, subject to the assumption that it is absolutely critical to observe the complete rotor dynamics. The enhanced technology incorporated in these sensor optimizations includes a Modal Filter for stochastic monitoring, a patented static blade deflection estimator based on centripetal acceleration, and order analysis for the deterministic monitoring of structural response. All of these methods are discussed by White[20] and White, Adams and Rumsey[21].

The performance of the instrumentation array of the SMART Rotor will be critical to the capabilities and performance of the active load control system; each rotor blade has been instrumented with an internally-mounted array of accelerometer, fiber-optic strain, metal foil strain and fiber-optic temperature sensors, as well as pressure taps and Pitot tubes. The number and locations of the accelerometers were driven by the sensor optimization strategies that account for expected rotor loads, deflections, modal contributions, mass and stiffness distributions, and co-locations with other measurements for multi-physics observers.

Applying these optimizations results in single triaxial and uniaxial accelerometers placed at the 2m and 8m locations in each blade to permit estimation of all linear deflections and span-wise rotations. The strain sensors are located at the root, 25%, 50%, and 75% of blade spanwise distance to enable accurate capture of the curvature along the blade for the application of shape reconstruction force and deflection estimators. The measurements at these locations will also be used to train a modal filter for the application of multi-physics observers. Single metal foil and fiber-optic strain gauges are mounted at each of these locations to enable comparison of the performance of the two technologies. SNL has been performing metal-foil strain measurements of operational rotor blades for nearly four decades, but these sensors have never demonstrated the long-term reliability that would be needed for utility application. Fiber-optic strain measurements, on the other hand, are a fairly recent application for SNL, but they have been shown to continue to perform well at cycle counts well above those which are expected in the 20-year life of a turbine rotor blade. The fiber-optic temperature sensors will be used to study the correlation between rotor blade temperature and structural performance; hopefully yielding crucial insight into the role of temperature in the “noise” or randomness that is typically observed in the strain signals recorded during online structural health and condition monitoring.

The aerodynamic measurements are installed at approximately 7.9m (the center spanwise location of the aerodynamic modules) on each blade. These measurements include a traditional five-hole Pitot tube for determining angle of attack and velocity (presently on only one blade), as well as an array of pressure taps to measure the chord-wise distribution of surface pressure. Two modifications were made to minimize the difficulties that past users of similar aerodynamic measurements have experienced. First, the Pitot tube was built with an integrated bend to place it at the nominal angle of attack orientation to maximize the angular range and accuracy of the measurement. Second, a highly accurate absolute pressure sensor was located in each blade to measure the reference pressure, eliminating the complexity associated with the pneumatic slip-ring required for the usual hub-mounted absolute pressure reference.

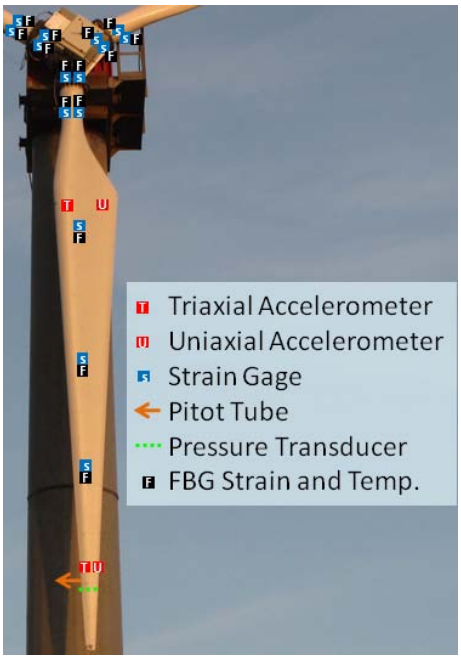

Figure 8 Schematic of Instrumentation on a 9m SMART Blade

Figure 8 is an illustration of the types and locations of sensors on the SMART blades.

An SNL team integrated these sensors into the SMART rotor blades prior to their closure during fabrication by TPI Composites. During this effort, the team evaluated and documented the problems and the lessons learned, capturing information that may prove to be relevant for future industry application of extensive sensor systems in rotor blades.

Previous sensor demonstration efforts by White, Adams and Rumsey[21] have shown that electrostatic discharge (ESD) is a field-test hazard that is a major contributor to sensor failure, particularly to accelerometers. The most well-known manifestation of ESD is lightning; to handle the large currents associated with lightning, a large copper cable has been installed inside each blade, connecting a lightning receptor located near the blade tip and the metal hub. This lightning protection was not present on the CX-100 blades, but is a common feature included in most wind turbine blades manufactured today. The ESD problems cited above, however, occurred mainly in the absence of lightning, most likely due to the triboelectric effect[22], the static build-up of charge due to the contact and separation of dissimilar materials. Air passing over turbine blades is an example of this effect; it can result in the accumulation of very large charges that can vary significantly along the blade, leading to discharges from one portion of the blade to another or to ground. Three features have been included in the SMART blades in an attempt to address this issue. First, fine wire mesh was added to the outside of the carbon laminate and a conductive gelcoat coating was applied to the entire blade surface at the time of fabrication. Both are grounded via the lightning protection cable. Also, while not intentionally designed in as an ESD mitigation mechanism, the conductive carbon fiber laminates in the outboard 2-meters in each blade do provide ESD dissipation. Second, more robust accelerometers with a much higher tolerance to ESD than those used in the prior efforts were used. Third, the accelerometers were mounted on orientation/grounding blocks that serve the dual purposes of orienting the sensor accurately and grounding the blocks via a cable connected to the blade root.

Measurement of these signals required the development of a rugged and robust hub-mounted data acquisition system. The new measurement system acquires precisely time-synchronized data (GPS based) from both ATLAS[23] and National Instruments Compact-RIO data acquisition systems and from additional Ethernet based instrumentation (the fiber optic and aerodynamic pressure measurements). These data are low-pass filtered, decimated, and transmitted wirelessly to a control building over 400 feet away. The system includes lightning protection to protect all acquisition, power, and communication channels and a battery backup to allow for safe and orderly shutdown of the system in case of power failure.

While all of these instrumentation and data acquisition improvements have been developed specifically for the existing SMART Rotor Experiment, many of the developments and lessons learned may be immensely valuable as the industry begins to adapt this technology for routine turbine application. The operational monitoring system developed for the sensor array is powerful for a controls observer, but also provides a foundation for new techniques for monitoring of rotor performance and structural health. This technology may be used in the future to estimate current loads and state of damage in order to predict the future life of the rotor based on damage growth models, developments that may ultimately enable improved turbine performance and optimal turbine operation and maintenance, helping to make wind energy more cost-competitive and offshore wind energy applications economically viable.

V. Reduced Order Model System Identification and Control System Design

System identification of an operating wind turbine, as opposed to the parked wind turbine structure, is meaningful in that it accounts for dynamic effects due to rotor rotation and aerodynamic loads and damping. A challenge in system identification of an operating wind turbine is in designing inputs that excite the dynamics of

interest in the turbine structure. A general process will be employed for the system identification for a Reduced Order Model (ROM) and Multi-Input Multi-Output (MIMO) control design of the operating SMART turbine. The main steps outlined here are required to adequately characterize a nonlinear aeroservoelastic system during operation and design a control architecture that includes effects of the most important dynamics contributing to the system behavior. This process is equally useful for numerical simulation of aerodynamically loaded wind turbines and for characterization and control design of a real wind turbine with active aerodynamic devices.

An advantage of numerical simulation is the easy access to simulated sensors for input and output purposes. A disadvantage of numerical simulation is the degree of confidence in the physical models and assumptions that are used in the simulation. Initially, an ADAMS/Simulink co-simulation tool will provide an opportunity to prove out processes prior to actual field implementation. The ADAMS/Simulink co-simulation environment provides a high fidelity structural and aerodynamic capability which, for example, will include unsteady aerodynamic active flap models. Open loop tests will be performed to confirm functionality and to excite critical dynamics used to build calibrated models. These calibrated models will serve as a foundation for the development of ROM sufficient for MIMO control design, implementation, and validation. Initial feedback control system design will include both classical (PD and PID) control and modern model-based control. Future work will deal with highly optimized controllers which have the ability to affect the dynamics of a system in an efficient manner that is subject to a cost function metric.

A mathematical model that adequately captures the systems dynamical motion is necessary for a successful controller design. System realization is the process of building a state-space model from experimental data and is an integral part of system identification and model accuracy[24]. The method of identifying the plant models, as well as the process and sensor noise statistics, initially utilized for this project will be the Observer/Kalman filter IDentification (OKID) method[24-26]. This method of system identification uses only input and output data to construct a discrete-time state-space realization of the system. The OKID method is well suited for MIMO systems and, by definition, the generated model matches the output in a least squares sense[25].

The OKID algorithm includes an observer in the system identification process. The first step in the process calculates observer Markov parameters that are assembled into a generalized Hankel matrix[25,27]. The next step employs a least squares technique to compute the system Markov parameters from which the observability, controllability, and state transition matrices can be determined[25]. In the final step, the Markov parameters are used to generate the discrete-time state-space model via the Eigensystem Realization Algorithm (ERA). At this point, an observer is added to the linear system equations and the system stability is established through augmentation of the ideal Markov parameters with that observer[27].

Specific open-loop data sets will be created that correspond to several wind conditions and excitation of wind turbine dynamics. Different combinations of chirp signals will be applied as inputs and the corresponding sensor signals recorded as outputs. These data files will be used as input for OKID to identify the dynamic characteristics of the model. The number of actual modes identified becomes a function of the richness of excitation in the data sets. The resulting observer model will then be employed in the control system design (as an example of the OKID process, see Figure 9).

The last step in the process will be to design the closed-loop feedback controller. For the initial, modern, model-based controller design, a standard LQR methodology[28] coupled with the identified state estimator from the OKID method will be employed. A LQR controller is determined from a quadratic cost function[27,28] that minimizes the weighted sum of the identified states and the control effort (limited by the maximum actuator control authority hardware constraints). By adjusting these weights (the LQR control design parameters), varying controller performances will result. The solution to the LQR minimization is the state feedback gain matrix K. Given that the implementation includes the OKID estimator, then at any given time-step, the control law is calculated from the *current estimate as*

$$u_k = -K\hat{x}_k$$

and the estimator is propagated forward in time using the current control and measured system outputs as

$$\hat{x}_{k+1} = [A + GC]\hat{x}_k + [B + GD]u_k - Gy_k$$

where $\hat{x}_{k+1}$ is the future state estimate, $\hat{x}_k$ the current state estimate, u_k current flap actuator command, y_k the current sensor (local flap deflection rate) measurements, and G the observer gain. This formulation will be implemented in the flap control module in the SMART rotor blade hardware and performance tests will be conducted.

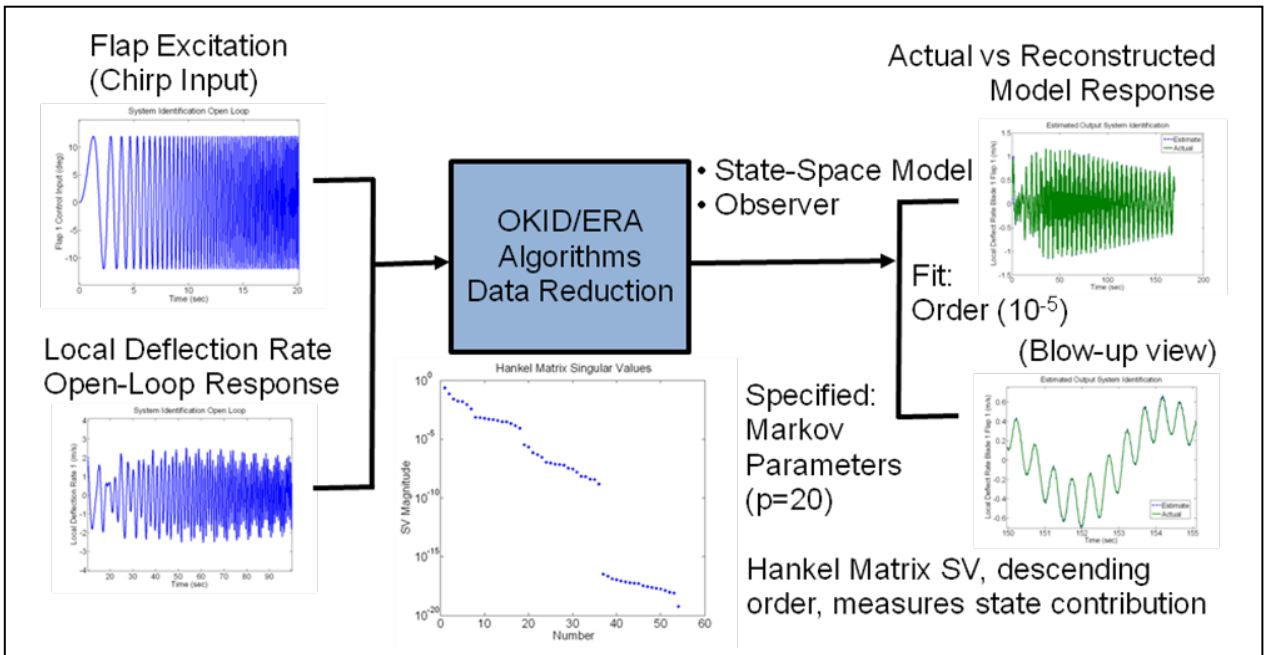

Figure 9 OKID Procedure using a 5MW UpWind Reference Wind Turbine Model and the DU_SWAMP Aeroservoelastic Wind turbine Simulator to Create the Input Data used to Identify the ROM for Modern Model-based Controller Design (from reference 16).

VI. Future Work

In the immediate future, initial testing will include "open-loop" testing to: 1) investigate conventional flap actuator functionality and 2) acquire data for all signals (reference and feedback) to establish sampling time, stability, and performance requirements. The primary goal of this testing will be to collect enough data to support system identification, reduced-order-model development for control design, and model validation of wind turbine structural and aerodynamic static and dynamic effects within conventional modeling tools such as FAST and ADAMS.

Future objectives and goals for the SMART rotor project will include the following activities:

1) Applicable techniques for system identification of the operational aeroservoelastic wind turbine in stochastic inflow conditions will be determined. This will be the first step in the process of understanding necessary system dynamics and then making appropriate choices regarding what to include in the implementation of a control scheme. The operational modes of the wind turbine are expected to be quite different from what can be measured on the parked turbine system due to effects of rotor rotation, aerodynamic loads and damping. Critical measurements of operational modes with the use of the appropriate rotor excitations will enable robust controller designs. This design can then be integrated within a smart health monitoring and overall wind turbine control system architecture.
2) Further investigations of load reduction under varying wind conditions using distributed flaps and various combinations of sensor measurements will be assessed. Studies of multiple flaps, flap spanwise locations, and sensor measurements (structural: strain, strain-rate, tip deflection, acceleration, surface pressure, angle of attack, etc.) can then be conducted to help identify promising active aerodynamic load control techniques. Trade-off studies of loads reduction and effects on energy capture will help develop the performance-optimized smart wind turbine system for the future.

Acknowledgments

The authors gratefully acknowledge the contributions of Michael Zuteck of MDZ Consulting and Joshua Paquette of SNL to the design of the SMART blades and of Gary Fischer of SNL to the early design of the active aerodynamics hardware.

References

[1]Barlas, T.K. and van Kuik, G.A.M., Review of state of the art in smart rotor control research for wind turbines, *Progress in Aerospace Science (2009)*, doi:10.1016/j.paerosci.2009.08.002

[2]van Wingerden, J-W., Hulskapp, A.W., Barlas, T., Marrant, B, van Kuik, G.A.M., Molenaar, D-P, and Verhaegen, M., On the Proof of Concept of a 'Smart' Wind Turbine Rotor Blade for Load Alleviation, Wind Energy, 2008; 11:265-80.

[3]Barlas, T., van Wingerden, J-W, Hulskamp, A, and van Kuik, G, "Closed-loop Control Wind Tunnel Tests on an Adaptive Wind Turbine Blade for Load Reduction," *Proceedings of the 46th AIAA/ASME*, Reno, NV, USA, 2008.

[4]Troldborg, N., Computational study of the Risø B1-18 airfoil with a hinged flap providing variable trailing edge geometry. *Wind Engineering* 2005, 29:89-113.

[5]Buhl, T., Gaunaa, M., and Bak, C., "Load reduction potential using airfoils with variable trailing edge geometry," *Proceedings of the 43th AIAA/ASME*, Reno, NV, USA, 2005.

[6]Buhl, T., Gaunaa, M., and Bak, C., Potential load reduction using airfoils with variable trailing edge geometry. *Solar Energy Engineering* 2005, 127:503-16.

[7]Andersen, P. B., Gaunaa, M., Bak, C., and Buhl, T., "Load alleviation on wind turbine blades using variable airfoil geometry," *Proceedings of the EWEC* 2006, Athens, Greece.

[8]Andersen, P. B., Gaunaa, M., Bak, C., and Buhl, T., "Wind tunnel test on wind turbine airfoil with adaptive trailing edge geometry," *Proceedings of the 45th AIAA/ASME*, Reno, NV, USA, 2007.

[9]Buhl, T., "Stability Limits for a Full Wind Turbine Equipped with Trailing Edge Systems," European Wind Energy Conference, Marseille, France, 16-19 March, 2009.

[10]Anderson, P.B., "Load Reduction Using Pressure Difference on Airfoil for Control of Trailing Edge Flaps," European Wind Energy Conference, Marseille, France, 16-19 March, 2009.

[11]Wilson, D.G., Berg, D.E., Barone, M.F., Berg, J.C., Resor, B.R., and Lobitz, D.W., "Active Aerodynamic Blade Control Design for Load Reduction on Large Wind Turbines" European Wind Energy Conference, Marseille, France, 26-19 March, 2009.

[12]Berg, D.E., Wilson, D.G., Barone, M.F., Berg, J.C., Resor, B.R., Paquette, J.A., and Zayas, J.R., "The Impact of Active Aerodynamic Load Control on Fatigue and Energy Capture at Low Wind Speed Sites", European Wind Energy Conference, Marseille, France, 16-19 March, 2009.

[13]Berg, D.E., Wilson, D.G., Resor, B.R., Barone, M.F., Berg, J.C., Kota, S. and Ervin, G., "Active Aerodynamic Blade Load Control Impacts on Utility-Scale Wind Turbines", WINDPOWER 2009, Chicago, Illinois, 5-7 May, 2009.

[14]Wilson, Berg, D.E., D.G., Resor, B.R., Barone, M.F., and Berg, J.C., "Combined Individual Pitch Control and Active Aerodynamic Load Controller Investigation for the 5MW UpWind Turbine, WINDPOWER 2009, Chicago, Illinois, 5-7 May, 2009.

[15]Resor, B., Wilson, D., Berg, D., Berg, J. , Barlas, T., and van Kuik, G., "The Impact of Higher Fidelity Models on Active Aerodynamic Load Control Fatigue Damage Reduction", *Proceedings of the 48th AIAA Aerospace Sciences Meeting*, Orlando, FL, January 4-7, 2010.

[16]Wilson, D.G., Resor, B.R, Berg, D.E., Barlas, T.K., and van Kuik, G.A.M., "Active Aerodynamic Blade Distributed Flap Control Design Procedure for Load Reduction on the UpWind 5MW Wind Turbine," *Proceedings of the 48th AIAA Aerospace Sciences Meeting*, Orlando, FL, January 4-7, 2010.

[17]Berg, D. E., Wilson, D., Resor, B., Berg, J., Barlas, T., Crowther, A. and Halse, C., "System ID Modern Control Algorithms for Active Aerodynamic Load Control and Impact on Gearbox Loading", The Science of Making Torque from Wind, 2010.

[18]Berry, D. and Ashwill, T., "Design of 9-Meter Carbon-Fiberglass Prototype Blades: CX-100 and TX-100", SAND2007-0201, September 2007, Sandia National Laboratories, Albuquerque, NM.

[19]NWTC Design Codes (PreComp by Gunjit Bir). http://wind.nrel.gov/designcodes/preprocessors/precomp/. Last modified 26-March-2007; accessed 26-March-2007.

[20]White, J. "Operational Monitoring of Horizontal Axis Wind Turbines with Inertial Measurements," Ph.D. Dissertation, Purdue University, West Lafayette, IN., 2010.

[21]White, J., Adams, D., Rumsey, M., "Measurement of Operational Loading and Deflection with a Smart Turbine Rotor Blade," WINDPOWER 2009, Chicago, IL, May 4-7, 2009.

[22]Triboelectric Effect: http://en.wikipedia.org/wiki/Triboelectric_effect

[23]Zayas, J., Jones, P., and Ortiz-Moyet, J.,"Accurate GPS Time-Linked Data Acquisition System (ATLAS II) User's Manual", SAND2004-0481, February 2004, Sandia National Laboratories, Albuquerque, NM.

[24]Juang, J.-N. and Pappa, R.S., "An Eigensystem Realization Algorithm for Modal Parameter Identification and Model Reduction," Journal of Guidance, Control and Dynamics, Vol. 8, No. 5, Sept.-Oct., 1985, pp. 620–627.

[25]Juang, J.-N., Applied System Identification, Prentice Hall PTR, Upper Saddle River, NJ, 1994.

[26]Juang, J.-N., Horta, L.G., and Phan, M., "User's Guide for System/Observer/Controller Identification Toolbox," NASA Technical Memorandum 107566, 1992.

[27]Elkaim, G.H. “System Identification-Based Control of an Unmanned Autonomous Wind-Propelled Catamaran,” Control Engineering Practice 17 (2009), pp. 158–169.
[28]Bryson, Jr., A.E. and Ho, Y.-C., Applied Optimal Control, Hemisphere Publishing Corp., New York, 1975.